III European Conference on Computational Mechanics
Solids, Structures and Coupled Problems in Engineering
C.A. Mota Soares et.al. (eds.)
Lisbon, Portugal, 5–8 June 2006

CONFIGURATIONAL DERIVATIVE AS A TOOL FOR IMAGE SEGMENTATION

Ignacio Larrabide [1], **Raúl A. Feijóo**[1], **André A. Novotny**[1] **and Edgardo A. Taroco**[1]

[1]LNCC - Laboratório Nacional de Computação Científica
Rua Getúlio Vargas 333 - CEP: 25651-075
Petropólis - RJ - Brazil
{nacho, feij, novotny, etam}@lncc.br

Keywords: Configurational derivative, image segmentation, segmentation quantitative evaluation.

Abstract. *The introduction to medicine of techniques coming from areas like Computational Fluid Dynamics, Structural Analysis, and Inverse Problems, made the use of imaging data such us Computed Tomography (CT), Magnetic Resonance Imaging (MRI), Single Photon Emission Tomography (SPECT), Positron Emission Tomography (PET) and Ultrasound (US) mandatory in order to apply this techniques to patient specific data. The process of identifying the different tissues and organs, called segmentation, is a maior concern in this analysis. This process can be tedious and time consuming when done by hand, so its been an early concern in image processing to automatize it. Many contributions have been made to this area since the introduction of the Mumford and Shah functional. This functional is endowed to quantify the* cost *associated to a specific segmentation.*

Our aim in this paper is to present an image segmentation method based on the configurational derivative of the cost functional $\mathcal{F}$ endowed to the image data. The configurational derivative can be viewed as an extension of the well established concept of topological derivative when, instead of a hole, a small inclusion is introduced at a certain point of the domain. Some results are presented in order to show the computational performance of this methodology in the presence of white Gaussian noise.

1 INTRODUCTION

Medical imaging techniques such as Computed Tomography (CT), Magnetic Resonance Imaging (MRI), Single Photon Emission Tomography (SPECT), Positron Emission Tomography (PET) and Ultrasound (US) provide useful information (anatomical and functional) to the specialists, no matter what area are they from (medicine, research, etc.). Consequently, the demand for tools to manipulate these images has grown considerably since the appearance of these technologies. Over the years different issues have appeared in the area of medical image processing, to recall some of them we can mention image registration, volume data visualization, image segmentation and enhancement, pattern recognition among others.

These data sets provide information otherwise unavailable for clinical specialists to analise. Quantitative information such as organ size and shape can be extracted from these images in order to support activities such as disease diagnosis and monitoring and surgical planning. However, in order to accomplish this, the first step we must do is to identify the different tissues and anatomical structures being involved. This process, called segmentation, must be accurate and repeatable in order to be clinically useful.

Segmentation is the process that subdivides an image into its constituent regions or objects. The level to which the subdivision is carried depends on the problem being solved. For example, in the segmentation of medical images, the objective is usually to identify different regions, organs and anatomical structures from imaging data.

The inherent complexity of these areas has motivated interdisciplinary research and the use of techniques actually born in other areas into medicine as well as image processing. The introduction of technologies like Configurational derivative, originally conceived for the study of topology optimization problems, has shown interesting results when applied to image processing[10, 17].

Classical image segmentation techniques are based on two basic pixel[1] characteristics: discontinuities and similarities. Many of this classical techniques (e.g., multiple thresholding, region growing, morphologic filtering and others [3, 5]) have been applied to try to solve this problem with variable outcomes [14, 16]. Such techniques tend to be unreliable when segmenting a structure that is surrounded by others with similar image intensity (eg, low-contrast structures).

More sophisticated techniques, like Level Sets, use powerful numerical computations for tracking the evolution of moving surface fronts. These techniques are based on computing linear/nonlinear hyperbolic equation solutions for the appropriate equations of motion. An initial approximation of the solution (seed) evolves until it gets the limits of the region of interest. In this case user interaction is needed to introduce one or more seeds for the algorithm to evolve from [11, 19]. Although this approach brings good results, it's computational cost may become too high. A wide variety of works present the Active Contour (also called Snakes) technique as the most robust for medical image segmentation [4, 6, 9, 18]. With this technique good results are obtained, in particular for brain MRI segmentations, in this case input data must be pre-processed to extract spurious structures before the segmentation algorithm is started.

By means of Markov Random field in [15] and [21] are described fully automatic 3D-segmentation techniques especially designed for brain MRI images. This techniques captures three main spatial features of MRI images: non-parametric distribution of tissue intensities, neighborhood correlations and signal inhomogeneities. Once these fields are calculated (using suitable probabilistic models), an iterate optimization algorithm (Iterated Conditional Modes,

[1] By pixel we mean picture element.

Simulated Annealing, Expectation-Maximization, etc.) is used to recalculate them until the convergence is achieved. Again, the limitation of this technique is it's excessive computational cost.

Our aim in this paper is to quantitatively evaluate the outcomes of a recently introduced image segmentation method based on a discrete version of the well established concept of configurational derivative (see [1, 2, 8, 12, 13] and references therein). More specifically, we compute the configurational derivative for an appropriate functional associated to the image indicating the *cost* endowed to an specific image segmentation. Further, we propose an image segmentation algorithm based on this result. Several results for different levels of White Gaussian Noise (WGN) are presented in order to show the computational performance of this methodology. And finally, some medical images are segmented to show some possible applications of these methods.

2 FORMAL DEFINITION OF THE CONFIGURATIONAL DERIVATIVE

The configurational derivative allows us to quantify the sensitivity of the problem when the domain under consideration is perturbed by changing a material property at a specific point. More specifically, let Ω be an open set in $\mathbb{R}^N$ ($N = 2, 3$) and B_ε be a ball of radius ε centered at point $\tilde{x} \in \Omega$ (Figure 1). Taking into account a cost function Ψ, the associated configurational derivative D_C can be defined as:

$$D_C(\tilde{x}) = \lim_{\varepsilon \to 0} \frac{\Psi\left(\Omega_\varepsilon \cup \overline{B}_\varepsilon\right) - \Psi\left(\Omega\right)}{f\left(\varepsilon\right)} \,, \tag{1}$$

$$\Psi\left(\Omega_\varepsilon \cup \overline{B}_\varepsilon\right) = \Psi\left(\Omega\right) + f\left(\varepsilon\right) D_T(\tilde{x}) + \ldots \tag{2}$$

where $\Omega_\varepsilon = \Omega \backslash \overline{B}_\varepsilon$, $f\left(\varepsilon\right)$ is a negative valued function that decreases monotonically so that $f\left(\varepsilon\right) \to 0$ with $\varepsilon \to 0^+$. The configurational derivative D_C given by Eq. (1) has been recog-

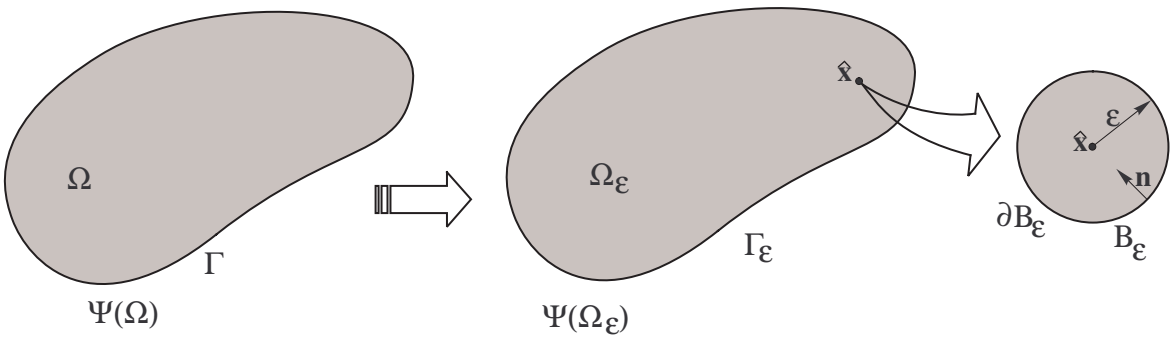

Figure 1: Configurational derivative concept.

nized as a powerful tool to solve topology optimization problems. Nevertheless, this concept is wider. For example, the topological derivative (a particular case of D_C, where the inclusion is repaced with a a vacuum) has been studied in order to consider arbitrary shaped holes and its applications to Navier, Laplace, Poisson, Helmoltz, Stokes, Navier-Stokes equations are developed by Masmoudi and by Sokolowsky and their co-workers. See also [1, 13, 20] for

applications of the topological and configurational derivative to the above equations, inverse problems and material properties characterization. As already mentioned in this paper, we will introduce a discrete version for the configurational derivative, which will be applied in the context of image segmentation.

3 IMAGE SEGMENTATION PROBLEM

In this work we deal with 2D images, therefore, the image will be characterized by a two-dimensional matrix of pixels[2]. For each image element (pixel) we associate an intensity according to the image type[3] and the technique used to acquire it. In addition, the image intensity is normalized assuming values from 0 to 1.

More specifically, let us consider a two-dimensional image characterized by an $M \times N$ matrix of pixels ω^{ij}. For each pixel ω^{ij} we respectively associate the intensities of the original image $u^{ij} \in \mathcal{U}$, and segmented image $\bar{v}^{ij} \in \mathcal{V}$, where the sets $\mathcal{U}$ and $\mathcal{V}$ are defined as:

$$\mathcal{U} := \{u^{ij} \in \mathcal{I} : i = 1...N,\ j = 1...M\}\ , \tag{3}$$

$$\mathcal{V} := \{v^{ij} \in \mathcal{C} : i = 1...N,\ j = 1...M\}\ . \tag{4}$$

Furthermore, the set $\mathcal{I}$ represents the normalized intensity values of the original image and the set $\mathcal{C}$ represents the intensities classes holding the solution of the segmentation. That is, the sets $\mathcal{I}$ and $\mathcal{C}$ are defined as:

$$\mathcal{I}{:=}\{\rho \in \mathbb{R} : 0 \leq \rho \leq 1\} \quad \text{and} \quad \mathcal{C}{:=}\{c_s \in \mathcal{I} : s = 1...Nc\}\ , \tag{5}$$

where Nc is the number of classes and c_s represents a given class.

To identify a class different alternatives can be used. The values defined for the classes will depend on the cost function and the specific application of the segmentation. Therefore, we will obtain different results according to the criterion adopted to define the set of classes $\mathcal{C}$ (for instance, mean intensity or median intensity inside a region). In this work the expected mean intensity value inside a region was used to define the class that represents that region. Other *a priori* image information can be used to determine this values. In the case of CT the brighter intensities represent bone and darker areas represent soft tissues as inner organs or muscles. This information can be used to determine classes's characteristic values and appropriate cost function for the problem under consideration.

Finally, the image segmentation problem studied here can be stated as following: given the original image represented by the matrix $u^{ij} \in \mathcal{U}$, the set of classes $\mathcal{C}$ and a specific cost function, find the segmented image represented by the matrix $\bar{v}^{ij} \in \mathcal{V}$ such that minimizes the cost function.

3.1 Choosing the Cost Function

The election of the cost function depends on each particular problem. In this case we are interested in detecting different objets. In order to do this we could, for instance, characterize different objects by an intensity value characterizing the region occupied by that object. This characteristic intensity value is tightly related to the cost function being used. In this case, the following cost function was used:

$$\Psi = \theta\Phi + (1-\theta)\Gamma\ , \quad \text{with} \quad \theta \in (0,1] \subset \mathbb{R}\ , \tag{6}$$

[2]This algorithm is also extensible to 3D images.

[3]RGB, Grayscale, 8bpp Grayscale, etc.

where the first terms of the cost function Ψ, denoted by Φ, is associated to the *distance* between the input image pixel's intensities u^{ij} and the (in between iterations) segmented image intensities v^{ij}. The second term Γ quantifies the *contour measure* for every region. In particular, for this discrete case, these functions can be written as:

$$\Phi \;=\; \sum_{ij}(u^{ij}-v^{ij})^2 \quad \text{and} \quad \Gamma \;=\; \frac{1}{4n}\sum_{ij}\chi(v^{ij})\;, \tag{7}$$

where n is the number of dimensions where the segmentation is being done and $\chi(v^{ij})$ is a characteristic function that assumes the values 1 (one) over the boundary of pixels separating different classes and 0 (zero) otherwise. The θ parameter controls the contribution of each term Φ and Γ in the cost function.

3.2 The Configurational Derivative Computation

Next, it is computed the sensitivity of the cost function when the intensity of an arbitrary pixel $\omega^{\alpha\beta}$ is changed from class $v^{\alpha\beta}$ to class c_s. Therefore, the perturbed cost function Ψ_s is given by:

$$\Psi_s \;=\; \theta\Phi_s + (1-\theta)\Gamma_s\;, \tag{8}$$

where Φ_s and Γ_s can be written as:

$$\Phi_s \;=\; \Phi - (u^{\alpha\beta}-v^{\alpha\beta})^2 + (u^{\alpha\beta}-c_s)^2\;, \tag{9}$$

$$\Gamma_s \;=\; \Gamma - \frac{1}{4n}\left(\chi(v^{\alpha\beta}) - \chi(c_s)\right)\;, \tag{10}$$

Then the sensitivity, characterized by the configurational derivative, in this discrete case is given by the difference $\Psi_s - \Psi$, that is:

$$D_C^s(\omega^{\alpha\beta}) = \theta\left[(u^{\alpha\beta}-c_s)^2 - (u^{\alpha\beta}-v^{\alpha\beta})^2\right] + (1-\theta)\frac{1}{4n}\left[\chi(c_s)-\chi(v^{\alpha\beta})\right]. \tag{11}$$

$$D_T^s(\omega^{\alpha\beta}) = \Psi(\omega^{\alpha\beta}\backslash c_s) - \Psi(\omega^{\alpha\beta}). \tag{12}$$

3.3 An Image Segmentation Algorithm

In this section is presented a configurational derivative segmentation algorithm for a 2D image (Algorithm 1). The algorithm inputs are the 2D image $u^{ij} \in \mathcal{U}$ to be segmented and a set of classes in witch image pixels will be classified. The algorithm output is $\bar{v}^{ij} \in \mathcal{V}$, corresponding to the class that pixel ω^{ij} was classified. In fact, the configurational derivative can be used as a descent criterion in an optimization process. Then, the sufficient local minimum condition for such pixel perturbation is given by:

$$D_C^s(\omega^{\alpha\beta}) \geq 0 \quad \forall\, \alpha = 1,\ldots,N\;,\; \beta = 1,\ldots,M \; and \; s = 1,\ldots,Nc \tag{13}$$

Moreover, this algorithm consists in evaluating the configurational derivative for each pixel and each class. Then, the new (segmented) image is obtained by successively selecting for each pixel the class which produces the most negative value of the D_C at that pixel.

Is easy to notice that the result will be greatly influenced by the values determined for the different classes. In this case, every class has approximately the mean value of the pixels corresponding to that region.

Algorithm 1 Image segmentation based on a discrete version of the Configurational Derivative

Require: A 2D image $u^{ij} \in \mathcal{U}$, the set of classes $\mathcal{C}$, and $\theta^* \in (0, 1]$
Ensure: The segmented image $\overline{v}^{ij} \in \mathcal{V}$
  normalize the image and classes values
  take $\theta = 1$
  for every pixel $\omega^{\alpha\beta}$ **do**
    for every class $c_s \in \mathcal{C}$ **do**
      compute $D_C^s(\omega^{\alpha\beta})$ following (eq. 12)
    end for
    if $\min\{D_C^s(\omega^{\alpha\beta}),\ s = 1, \ldots, N_c\} < 0$ **then**
      $v^{\alpha\beta} = c_s$
    end if
  end for
  take $\theta = \theta^*$
  while $\exists\ s$ and $\alpha\beta$ such as $D_C^s(\omega^{\alpha\beta}) < 0$ **do**
    for every pixel $\omega^{\alpha\beta}$ **do**
      for every class $c_s \in \mathcal{C}$ **do**
        compute $D_C^s(\omega^{\alpha\beta})$ following (eq. 12)
      end for
      if $\min\{D_C^s(\omega^{\alpha\beta}),\ s = 1, \ldots, N_c\} < 0$ **then**
        $v^{\alpha\beta} = c_s$
      end if
    end for
  end while

As was mentioned above, the cost function has two terms, one measuring the distance between pixel intensities and a second one that measures the boundary of the different regions. Depending on the case, the cut condition used in Algorithm 1 may never be true[4]. For this reason a different stoping criterium was implemented. A tolerance was determined based on the initial value of the cost function (say $\Psi_s * 10^{-8}$ for the initial image). When the cost function value decrease between two consecutive iterations is below this value, the algorithm stops.

In order to give stability to the method, a fixed point algorithm was used to select the new class value for the segmented image in every new iteration. This consists in taking only a part of the values that the configurational derivative points out to be changed (pixels presenting a negative configurational derivative). In some cases (when the level of noise is too high for example) changing **all** the pixels whose configurational derivative is negative shields an oscillating result, that is, the step size is too big. This phenomenon produces very bad quality segmentation (if it converges at all!). To avoid this unwanted behavior, only a percentage of the pixels that have a negative D_C value are re-classified. For the numerical results presented in the next section, only the 50% of the pixels that had the most negative D_C were changed in every iteration. This simple technique stabilizes the algorithm and produced a convergent result in all the cases.

4 NUMERICAL RESULTS

The main objetive of the numerical tests is to evaluate the algorithm's effectiveness in the presence of noise. With this in mind, different test cases were build. A synthetic image com-

[4]It might happen, for a specific image, that in every iteration exists a pixel $\omega^{\alpha\beta}$ for whom $D_C^s(\omega^{\alpha\beta}) < 0$.

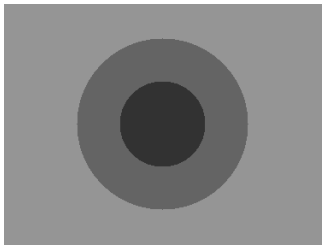

Figure 2: Synthetic image.

posed of two concentric circles was build, this image presents three different grayscale intensities (Fig. 2). Different levels of noise were applied in order to test the behavior of the algorithm. The applied noise is WGN with zero mean and different levels of variance. The variance of the noise goes from 0.01 to 0.2, in steps of 0.01. Each variance gives a different testing case. After the synthetic image is degraded using noise, a convolution with a smoothing kernel is used to smooth the image in order to leave the image as real as possible[5]. As we dispose of the ground truth segmentation (the original synthetic image), we are able to measure the algorithm's accuracy.

4.1 Methodology

In Figure 4 different results are presented. To obtain tese different test cases WGN with different variances (0.01, 0.05, 0.1, 0.15 e 0.2 respectively) was used. In order to be able to simulate a real image, a convolution with a Gaussian 5x5 kernel was applied twice over every image. This makes the image more real.

The metrics [7, 22] used to compare the results of the proposed algorithm with the ground truth image (Figure 2) were the following:

- **Tanimoto index:** This index is calculated as

$$I(A_1, A_2) = \frac{n(A_1 \cap A_2)}{n(A_1 \cup A_2)} \tag{14}$$

  that is, the ratio between the quantity of pixels in the intersection of the original region A_1 and the corresponding region in the segmented image A_2, and the quantity of pixels in the union of both regions.

- **Overlap index:** Is defined as [22]:

$$O(A_1, A_2) = 2 \cdot \frac{n(A_1 \cap A_2)}{n(A_1) + n(A_2)} \tag{15}$$

  that is, the ratio between the quantity of pixels in the intersection of the original region A_1 and the corresponding region in the segmented image A_2, and the sum of the number of pixels in both regions.

- **Preservation of the center of mass:** This index is given by the distance (in pixels) between the centers of mass of the original region and its segmented counterpart respectively.

[5] Real systems usually produce a noise+smoothing effect.

- **Distance between borders:** This index is given by

$$D(C_1, C_2) = \frac{\sum_{i=1}^{np1} d(x_1^i, C_2) + \sum_{i=1}^{np2} d(x_2^i, C_1)}{np1 + np2} \tag{16}$$

where $d(x, C)$ means the distance (in pixels) of the point x to the curve C, C_1 and C_2 are the boundaries of the original and segmented region respectively, x_1^i and x_2^i denote arbitrary points on the boundaries C_1 and C_2, finally $np1$ and $np2$ are the number of points which characterize the respective boundaries.

In Figure 3 the behavior of each index with respect to noise level is presented. As expected, a loss in the segmentation quality is observed when noise raises. However, the algorithm still gets high quality results even in the presence of severe noise. In fact, the Tanimoto/Overlap index gives errors less than 5% for 0.20 variance WGN. Furthermore, the other two indices (preservation of the center of mass and distance between borders) shown deviations of the order of a half of a pixel for the same level of noise.

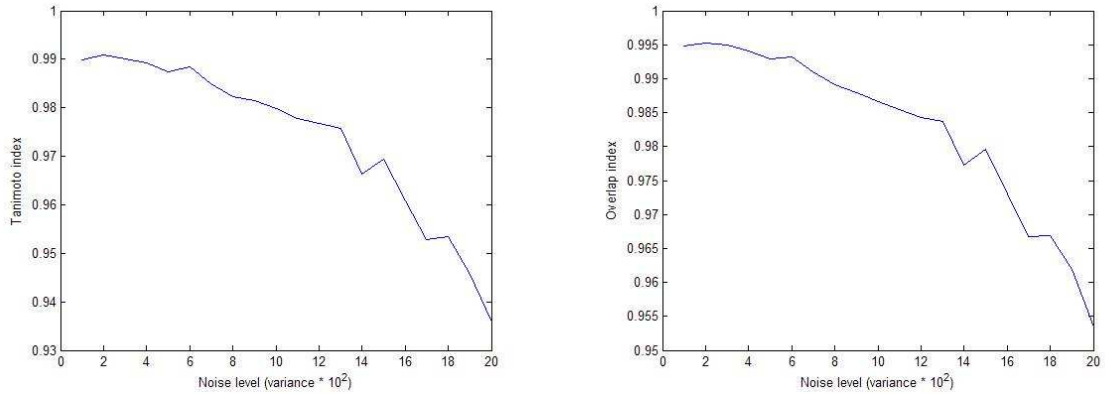

(a) Tanimoto index.

(b) Overlap index.

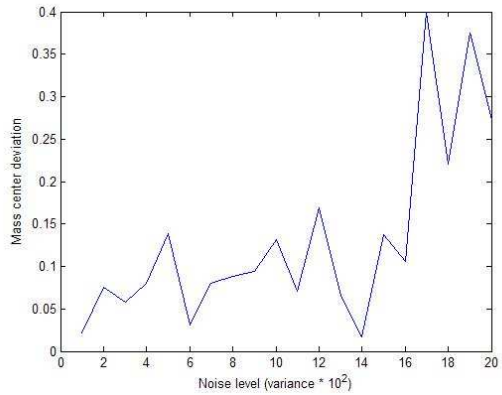

(c) Mass center deviation.

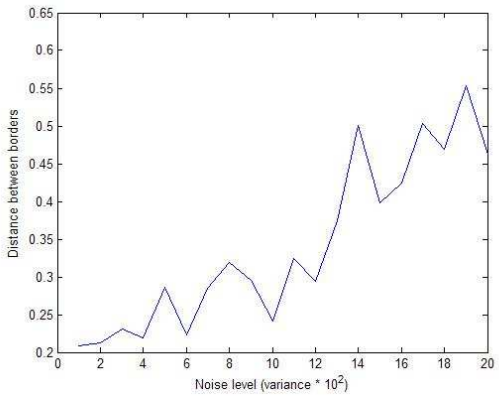

(d) Borders distance.

Figure 3: Behavior of the adopted indices

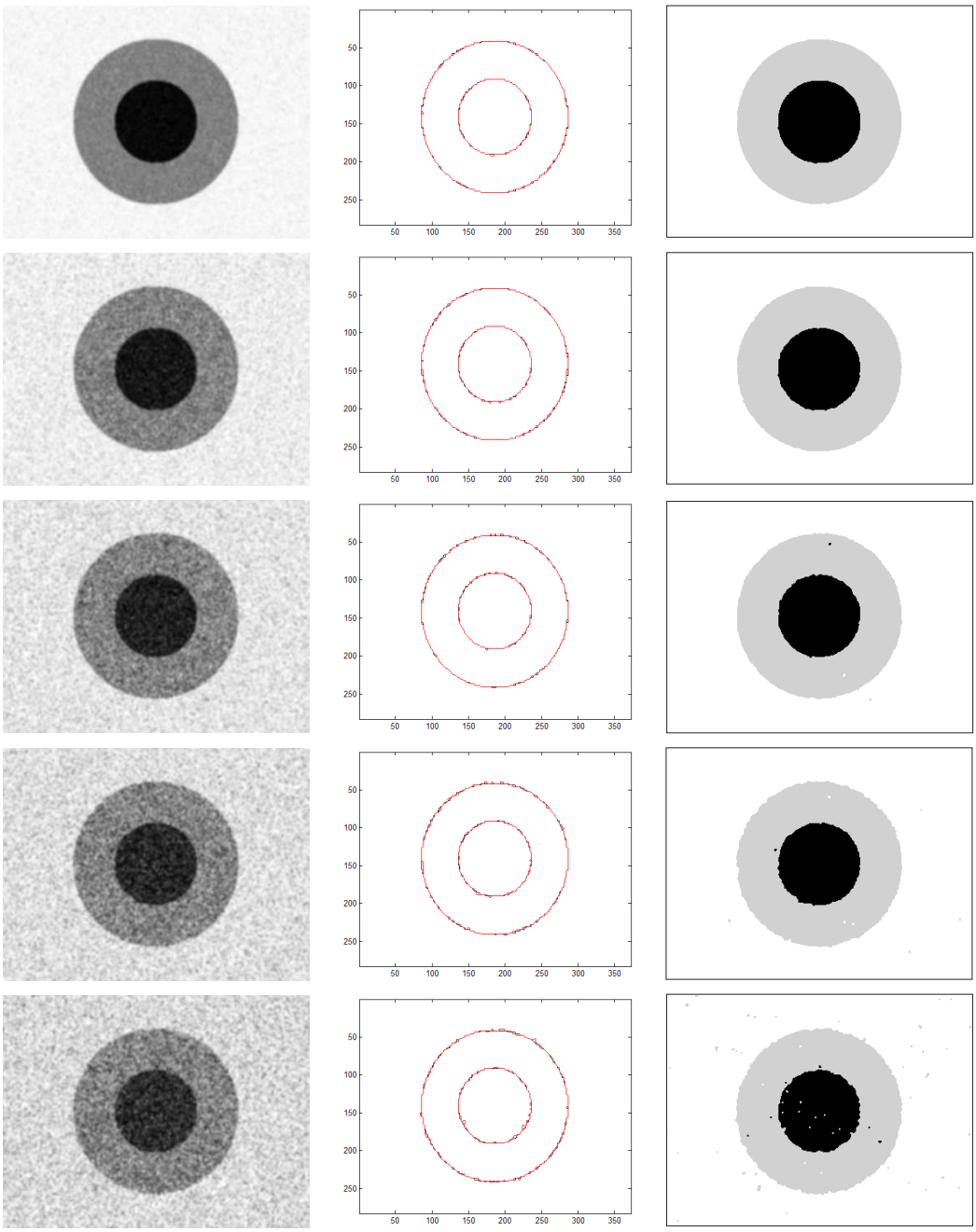

Figure 4: Segmentation results for different levels of noise. In this image the fist column corresponds to the image convolved two times with a Gaussian kernel matrix (5x5). The second column shows the boundaries of the original (black) and the segmented (red) regions respectively. The rows correspond to different levels of noise being 0.01, 0.05, 0.1, 0.15 and 0.2 the variances used.

5 CONCLUSIONS

In this work a segmentation algorithm based on the concept of Configurational Derivative was presented. The configurational derivative for an appropriate functional indicating the *cost* endowed to a specific image segmentation was also calculated. This algorithm was tested against images with different levels of noise. The outcomes revealed that even for high lev-

els of noise the segmentation method appears robust.

This algorithm is straight-forward to be implemented and produces good quality segmentations with very little additional information and almost no user interaction, besides the set of classes $\mathcal{C}$, for its initialization.

ACKNOWLEDGMENTS

This research was partly supported by the brazilian agencies CNPq/FAPERJ-PRONEX, under Grant E-26/171.199/2003. Ignacio Larrabide was partly supported by the brazilian agency CNPq (141336/2003-0). The support from these agencies is greatly appreciated.

REFERENCES

[1] A.A.Novotny. *Análise de Sensibilidade Topológica*. Phd thesis, Laboratório Nacional de Computação Científica, Petrópolis - RJ - Brazil, 2003.

[2] A.A.Novotny, R.A.Feijóo, C.Padra, and E.Taroco. Topological sensitivity analysis. *Computer Methods in Applied Mechanics and Engineering*, 192:803–829, 2003.

[3] A.K.Jain. *Fundamentals of Digital Image Processing*. Prentice Hall, 1989.

[4] Xu C., Pham D.L., and J.L.Prince. *Medical Image Segmentation Using Deformable Models*, pages 129–174. SPIE Handbook on Medical Imaging - Volume III: Medical Image Analysis, 2000.

[5] C.R.Gonzalez and R.E.Woods. *Digital Image Processing - Second Edition*. Prentice Hall, 2001.

[6] C.Xu, D.L.Pham, M.E.Rettmann, D.N.Yu, and J.L.Prince. Reconstruction of the human cerebral cortex from magnetic resonance images. *IEEE Transactions on Medical Imaging*, 18(6):467–480, 1999.

[7] F.Alonso, M.E.Algorri, and F.Flores-Mangas. Composite index for the quantitative evaluation of image segmentation results. In *Proceedings of the 26th Annual International Conference of the IEEE EMBS*, pages 1794–1797, San Francisco, CA, USA, 2004.

[8] H.A.Eschenauer, V.V.Kobelev, and A.Schumacher. Bubble method for topology and shape optimization of structures. *Structural Optimization*, 8:42–51, 1994.

[9] H.Li, R.Deklerck, B.DeCuyper, A.Hermanusa, E.Nyssen, and J.Cornelis. Object recognition in brain ct-scans: knowledge-based fusion of data from multiple feature extractors. *IEEE Trans. Med. Imaging*, 14:212–229, 1995.

[10] I.Larrabide, A.A.Novotny, R.A.Feijóo, and E.Taroco. A medical image enhancement algorithm based on topological derivative and anisotropic diffusion. In *Proceedings of the XXVI Iberian Latin-American Congress on Computational Methods in Engineering - CILAMCE 2005 - Guarapari, Esprito Santo, Brazil*, 2005.

[11] J.A.Sethian. *Level Set Methods and Fast Marching Methods*. Cambridge University Press, 1999.

[12] J.Céa, S.Garreau, Ph.Guillaume, and M.Masmoudi. The shape and topological optimizations connection. *Computer Methods in Applied Mechanics and Engineering*, 188:713–726, 2000.

[13] J.Sokolowski and A.Żochowski. On the topological derivative in shape optimization. *SIAM Journal on Control and Optimization*, 37:1251–1272, 1999.

[14] J.Suri, S.Singh, and K.Setarehdan, editors. *Advanced algorithmic approaches to medical image segmentation: state-of-the-art applications in cardiology, neurology, mammography and pathology*. Springer-Verlag, 2001.

[15] k.Held, E.R.Kops, B.J.Krause, W.M.Wells 3rd, R.Kikinis, and H.W.Muller-Gartner. Markov random field segmentation of brain mr images. *IEEE Trans. Med. Imaging*, 16(6):878–886, 1997.

[16] K.H.Hohne, H.Fuchs, and S.M.Pizer. *3D imaging in medicine: algorithms, systems, applications*. Springer-Verlag, New York, 1990.

[17] I. Larrabide, R.A. Feijóo, A.A. Novotny, E. Taroco, and M. Masmoudi. An image segmentation method based on a discrete version of the topological derivative. In *World Congress Structural and Multidisciplinary Optimization 6, Rio de Janeiro*. International Society for Structural and Multidisciplinary Optimization, 2005.

[18] R.Boscolo, M.S.Brown, and M.F.McNitt-Gray. Medical image segmentation with knowledge-guided robust active contours. *Radiographics*, 22(2):437–448, 2002.

[19] R.Malladi and J.A.Sethian. Level set methods for curvature flow, image enhancement, and shape recovery in medical images. In *Proc. of Conf. on Visualization and Mathematics*, pages 329–345, Germany, 1997. Springer-Verlag.

[20] S.Amstutz. *Aspects théoriques et numriques en optimisation de forme topologique*. Phd thesis., Institut National des Sciences Appliques de Toulouse, Frana, 2003.

[21] Y.Zhang, M.Brady, and S.Smith. Segmentation of brain mr images through a hidden markov random field model and the expectation-maximization algorithm. *IEEE Transactions on Medical Imaging*, 20(1):45–57, 2001.

[22] P. Zijdenbos, B.M.Dawant, R.A.Margolin, and A.C.Palmer. Morphometric analysis of white matter lesions in mr images: Method and validation. *IEEE Trans. Med. Imag.*, 13(4):716–724, December 1994.